

High Frequency Dynamic Properties of Natural Rubber

H.R. AHMADI*, K.N.G. FULLER* AND A.H. MUHR*

Directly measured data for high frequency dynamic properties of natural rubber at room temperature are presented. The two experimental techniques employed are first, forced non-resonance using a high frequency servohydraulic machine which allowed measurement up to 600 Hz and second, forced longitudinal vibration of a viscoelastic bar, a method extending the frequency range up to about 1500 Hz.

Close agreement is shown to exist between the direct measurement and other data, measured over a range of temperatures at low frequencies and transformed to high frequencies by applying the time-temperature equivalence principle. Some low frequency data in the literature, however, do not, when transformed, show such good agreement with the present direct measurements. These show that the dynamic modulus of unfilled NR is fairly constant at room temperature up to 1500 Hz, whereas its loss factor increases by a factor of 4 from 100 Hz to 1000 Hz.

Elastomers are increasingly being used by designers and engineers for applications such as vibration isolation and noise reduction where behaviour at high frequencies may be important. Hence, there is a growing demand for dynamic data for elastomers throughout the audio-frequency range (20 Hz to 20 kHz). Directly measured data are seldom available in the literature for frequencies above 50 Hz. Most published high frequency data¹ are inferred by transforming measurements at lower frequencies and low temperatures using the time-temperature equivalence principle².

Experiments carried out recently³ at frequencies between 10 Hz and 400 Hz have shown the loss factor for unfilled natural rubber vulcanisates at room temperature to rise significantly. This rise in loss factor contradicts previously reported high frequency data¹ obtained by the transform method. The reason for the discrepancy could be either inaccurate

original data or the inapplicability of the transform method.

This paper presents further data for the dynamic properties of NR vulcanisates measured directly at high frequency. Two techniques were used. In the first, double shear test pieces or compression buttons were deformed sinusoidally in a high frequency servohydraulic machine (Schenck VHF 7). In the second, a strip of rubber was excited longitudinally with an electromagnetic shaker; the dynamic properties were calculated from measurements of the acceleration at each end of the strip by means of the theory appropriate to wave propagation in a visco-elastic bar. The first technique allowed measurements to be made up to ~600 Hz, while the second technique extended the range to around 1.5 kHz. The paper also includes data on the dynamic properties obtained by applying the transform method to the results published in the Engineering Data Sheet⁴ (EDS) series.

*Malaysian Rubber Producers' Research Association, Brickendonbury, Hertford SG13 8NL, United Kingdom

Comparison of this transformed data with the direct measurements should enable the validity of the time-temperature equivalence to be assessed.

THEORY

Longitudinal Vibration Method

The theory for the propagation of compressive plane waves along a bar has been employed⁵ to measure the complex Young's modulus of linear visco-elastic materials at high frequency. Norris and Young⁶ have presented the equations describing longitudinal forced vibration of a visco-elastic rod with added end mass (Figure 1). The end mass, which may represent a detector (accelerometer), can influence the response significantly, and should not be neglected as some workers have done previously.

When a long bar is displaced harmonically by $U_o = \bar{U}_o e^{i\omega t}$ at one end (Figure 1), the time-dependent displacement at a point x

along the axis of the bar can be expressed as $[\bar{U}_o + \bar{U}(x)]e^{i\omega t}$, where $\bar{U}(x)$ is given by the solution to the equation:

$$\frac{d^2 \bar{U}(x)}{dx^2} + k^{*2} \bar{U}(x) = -k^{*2} \bar{U}_o \quad \dots 1$$

k^* , the complex propagation constant, is given by:

$$k^* = \left| \frac{\rho \omega^2}{E^*} \right|^{1/2}$$

where ρ is the mass density and E^* is the complex Young's modulus

$$E^* = E' + iE'' = E e^{i\delta}$$

E' and E'' being the in-phase and out-of phase moduli and δ being the phase angle. The phase velocity, c is equal to $(E/\rho)^{1/2} \sin(\delta/2)$. This is the velocity of points of constant phase within an infinite wave train. The solution to Equation 1 is

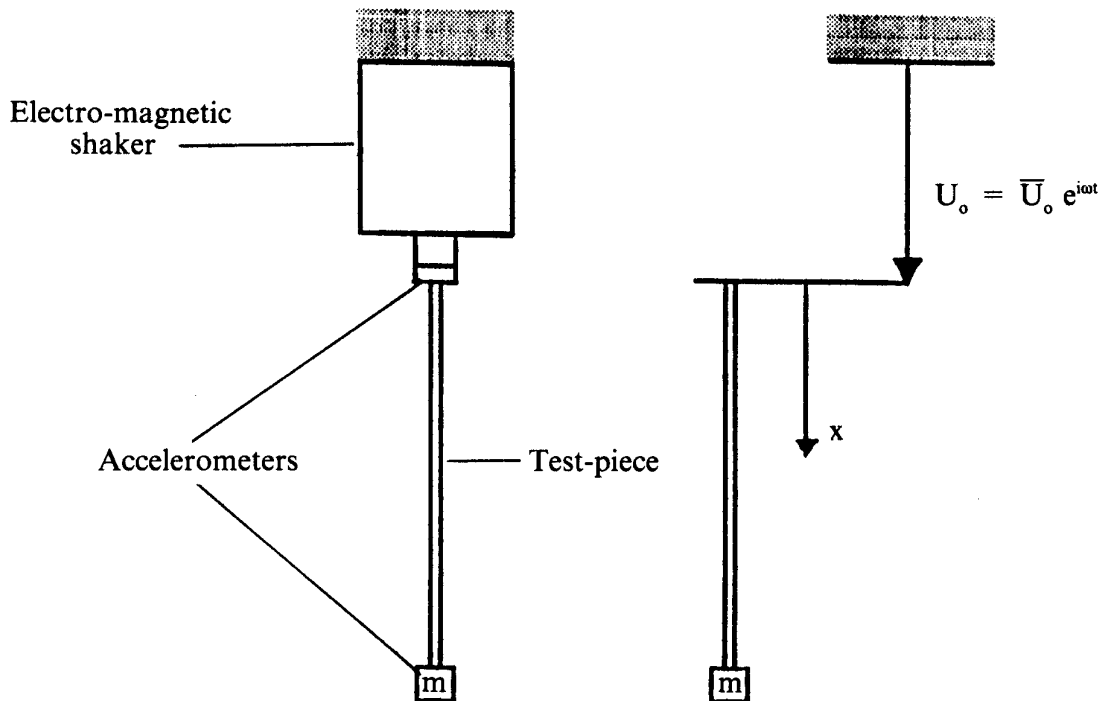


Figure 1. Schematic diagram of longitudinal vibration method.

$$\bar{U} + \bar{U}_o = C_1 \cos k^* x + C_2 \sin k^* x$$

C_1 and C_2 can be obtained from the boundary conditions:

$$\bar{U}(0) = 0$$

$$AE^* \left. \frac{\partial \bar{U}}{\partial x} \right|_{x=L} = m\omega^2 (\bar{U}(L) + \bar{U}_o)$$

where A and L are respectively the cross-sectional area and length of the bar, and m is the end mass. Substituting for C_1 and C_2 leads to:

$$\frac{\bar{U}(x)}{\bar{U}_o} = \cos k^* x + \left(\frac{\tan k^* L + \gamma}{1 - \gamma \tan k^* L} \right) \sin k^* x - 1$$

where $\gamma = k^* Lm/M$ and M is the mass of the rod.

The ratio, Q , of the peak acceleration at the free end to that at the driven end can be written as:

$$Q = \frac{\bar{U}(L) + \bar{U}_o}{\bar{U}_o} = \frac{1}{\cos k^* L - \gamma \sin k^* L}$$

$1/Q$ can be expressed in the form of real and imaginary parts

$$\frac{1}{Q} = \frac{\bar{U}_o}{\bar{U}(L) + \bar{U}_o} = Re + iIm$$

Defining 'the frequency ratio' ξ as:

$$\xi = \omega L/c = L 2\pi/\lambda$$

where λ is the wavelength and $R = m/M$ results in the expressions:

$$Re = \cosh \left(\xi \tan \frac{\delta}{2} \right) (\cos \xi - R \xi \sin \xi) + R \xi \tan \frac{\delta}{2} \cos \xi \sinh \left(\xi \tan \frac{\delta}{2} \right) \dots 2$$

$$Im = \sinh \left(\xi \tan \frac{\delta}{2} \right) (\sin \xi + R \xi \cos \xi) + R \xi \tan \frac{\delta}{2} \sin \xi \cosh \left(\xi \tan \frac{\delta}{2} \right) \dots 3$$

The magnitude of Re and Im are functions of the frequency of excitation and the dynamic properties of the material.

When the frequency is such that the phase angle between the acceleration at the driven end and that at the mass end of the bar is 90° , $Re = 0$ and $Im = |1/Q|$. It is interesting to note that when the end mass is zero (*i.e.* $R = 0$) such frequencies correspond to

$$\xi = \omega L/c = (2n + 1) \pi/2 \quad \text{where } n = 0, 1, 2, \dots \infty \quad \dots 4$$

$$\tan \frac{\delta}{2} = \frac{2 \sinh^{-1} (1/Q)}{(2n + 1) \pi} \quad \dots 5$$

the result obtained for the longitudinal modes of free-free rods with no end mass. In this work, the values of ξ and δ corresponding to solutions of *Equations 2* and *3* (with $Re = 0$ and Im equal to the measured value of $|1/Q|$) were obtained using a routine based on the Newton-Raphson method. For each mode the iteration was initiated according to *Equations 4* and *5*. Young's modulus and loss factor are given by:

$$E = \rho \left(\frac{\omega L}{\xi} \cos \frac{\delta}{2} \right)^2$$

$$\text{Loss factor} = \tan \delta$$

When the wavelength is of the same order as the lateral dimension of the sample, non-uniformity in the distribution of stress across the section of the sample becomes significant. Pochhammer and Chree⁷ provide an analysis for perfectly elastic rods when transverse planes can no longer be assumed to remain plane. There appears to be no comparable analysis for visco-elastic media. The analysis for perfectly elastic rods by Pochhammer and Chree suggests that when the wavelength is comparable to the lateral dimension of the sample the plane velocity c is no longer simply given by the 'bar velocity', $c_o = \sqrt{E/\rho}$. Instead, it becomes a function of the ratio of the smallest lateral

dimensions of the bar, d , to the wavelength, λ , the Poisson's ratio of the material, ν , and the bar velocity c_0 . The results of computations which give a value for c/c_0 for a given d/λ at the Poisson's ratio appropriate for rubbers ($\nu = 0.5$) are available⁸.

EXPERIMENTAL

Materials

The high frequency experiments were performed on two vulcanisates:

- A. An unfilled polybutadiene vulcanisate containing 0.5 p.p.h.r. of dicumyl peroxide
- B. An unfilled natural rubber vulcanisate similar to that used by Fletcher and Gent¹.

The low frequency data in the Engineering Data Sheet series⁴ were obtained on *Vulcanisates C* and *D*. The mix formulations and vulcanisation conditions for the test-pieces are given in *Appendix 1*. Polybutadiene was chosen because its low T_g (-113°C) should result in its dynamic properties at ambient temperatures remaining relatively constant over the range of frequencies used in the experiment. In order to assess the sensitivity of the experimental technique, the level of curative chosen gave a high crosslink density and hence a low loss factor.

Test-pieces

For longitudinal vibration tests, samples of *Vulcanisates A* and *B* were prepared by cutting strips of 5 mm width from moulded sheets 5 mm thick. The sample was bonded at each end to a miniature accelerometer (Kistler 8086A) with a mass of 0.5g.

Vulcanisate B was tested in the servo-hydraulic test machine using double shear test-pieces. The rubber was in the form of cylinders of 2 mm length and 25.4 mm diameter. For *Vulcanisate A*, the tests in the servo-hydraulic machine were carried out in compression using standard hardness buttons. The buttons (8 mm thick and

25.4 mm in diameter) were bonded at each end to light-weight aluminium plates. Their shape factor was 0.74, so that the compression modulus⁹ of the buttons was $(1 + 2S^2) E' = 2.1E'$.

High Frequency Test Methods

Forced non-resonance method. A servo-hydraulic machine, Schenck VHF 7 was used to deform the double shear test-pieces sinusoidally. A schematic diagram of the machine (showing transducer location) and test-pieces is given in *Figure 2*. The principle of this method is well documented¹⁰. The generator of a Solartron 1250 Frequency Response Analyser (FRA) provided the driving signal. The facilities of the FRA were utilised to analyse the signal from the piezo-electric force transducer and the displacement transducers. The transducer from which the displacement signal was taken switched from a linear variable differential transformer (LVDT) to a piezo-electric accelerometer at ~ 290 Hz. The results were obtained in terms of the ratio of the peak force to peak displacement signal at the driving frequency and their relative phase angle. The modulus and loss angle of the material were readily calculated as the stiffness of the grip connections and testing-machine were much higher than the sample stiffness. Correction for a known compliance of the test arrangement would have been straightforward.

The upper limit for the frequency of testing with this method is generally set by one of the following factors.

Resonance of the sample. The speed of shear waves for most rubbers at room temperature is about $25 - 35 \text{ ms}^{-1}$ and for a 2 mm thick sample the first resonant frequency, f , is $\sim 6 - 9$ kHz. As the driving frequency approaches sample resonance, the influence of the inertia of the sample can be observed as an increase in the apparent dynamic stiffness, K^* . In addition, the force signal gradually retards in phase and becomes out of phase with respect to the displacement signal.

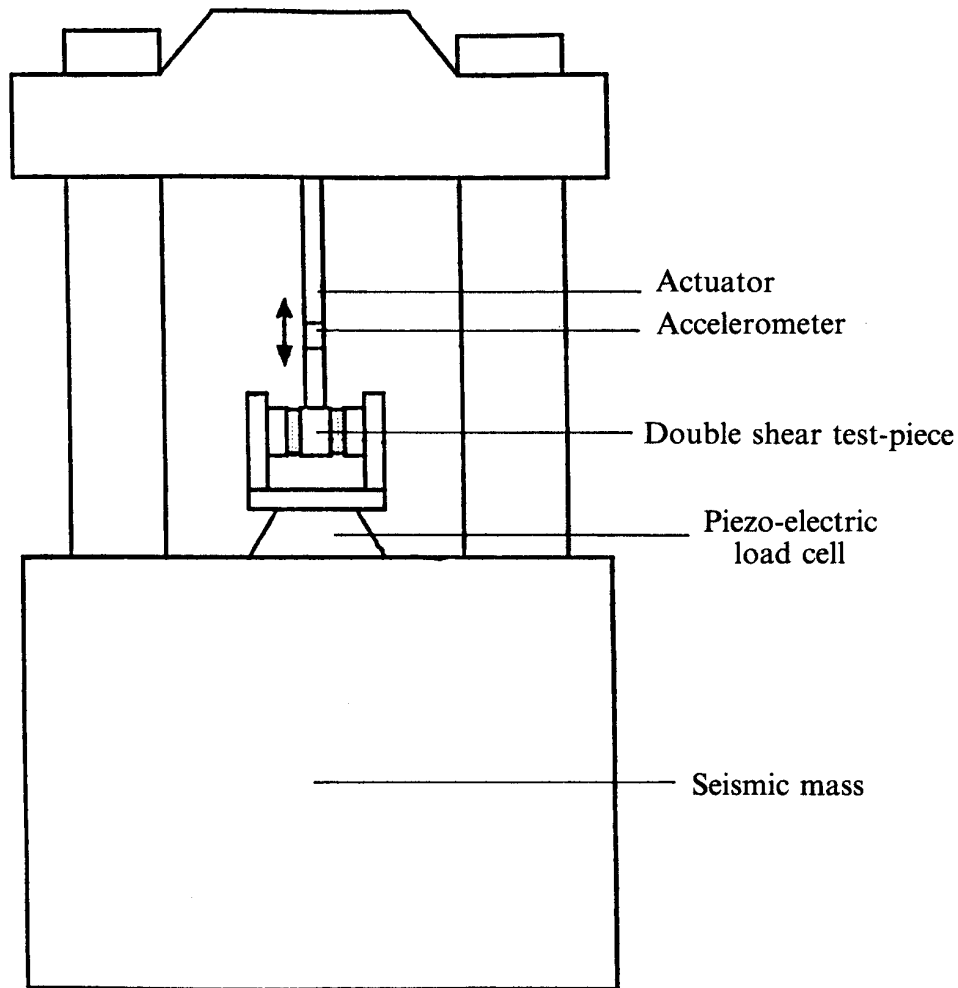


Figure 2. Schematic diagram of Schenck VHF 7 servohydraulic machine used in the forced non-resonance method.

The theory for the propagation of plane waves similar to those discussed above can be employed to quantify the error in the measured G^* and $\tan \delta$. It is shown (*Appendix 2*) that when the sample length is 5.5% of the wave length, the error in the modulus is $\sim 2\%$; the error rises to 7% when the length is 10% of the wave length. The first resonance occurs when the sample length is 50% of the wave length. For natural rubber at room temperature, a sample of 2 mm thickness gives 2% error at 800 Hz and 7% error at 1450 Hz. This compares to 265 Hz and 483 Hz for the 6 mm long sample recommended by BS903:A24¹¹.

For compression buttons, the first resonant frequency predicted by the theory for the propagation of compressive plane waves in slender rods is in the range of 2700 Hz to 3800 Hz. As the theory assumes that the ratio of the length of the sample to its diameter is $\gg 1$, while for the compression buttons $L/d \sim 0.3$, the figures should only be taken as approximate.

Resonance in the testing-machine or grip connection. The crosshead and column arrangement of the Schenck VHF 7 resonates at frequencies over 1 kHz. For example, when the crosshead is at its

highest position, the resonant frequency is ~ 1200 Hz. As a consequence the so-called 'seismic mass' of the machine moves in phase with the actuator, the amplitude depending upon the frequency. The error in the force signal from the load cell is proportional to the mass and amplitude of movement of the grip attached to it. For the Schenck VHF7, this is a significant artefact even though the load cell and grip are attached to a large seismic mass forming the base of the machine.

The effect was minimised by using light-weight alloys in construction of the jig. In order to find the frequency at which the effect of resonance was significant, a sample was placed in the lower grip, but the upper grip was not attached. The level of the force on the load cell was recorded for frequencies up to 1000 Hz, the amplitude of the actuator being $10 \mu\text{m}$. The upper grip was then connected and the sample tested with the same amplitude. The error in the force signal was found to reach 0.5% at a frequency between 450 Hz and 600 Hz depending on the stiffness of the test-piece.

Longitudinal vibration tests. The specimen is driven by an electro-magnetic shaker (Ling dynamics V201) as shown schematically in *Figure 1*.

A Solartron 1250 frequency response analyser (FRA) was used to provide the driving signal for the shaker and to analyse the signals from the accelerometers. The sweep and analysis facility of the FRA provided a means for quickly searching for the frequencies at which the acceleration at the driven end was 90° out of phase with that at the free end. The ratio of the accelerations, Q , close to each mode of longitudinal resonance was then obtained by fine tuning the input signal around those frequencies.

Typically, the length of the specimen was ~ 7 cm. Longer specimens were used

successfully, but for shorter specimens (< 5 cm), the larger mass ratio, R , increased the significance of any uncertainty in the contribution of the cable of the accelerometer to the end mass. The uncertainty could lead to significant errors in the case of the damping factor, particularly for higher modes.

A range of mass ratios R of 0.26 – 0.7 and up to 12 modes of the longitudinal resonance were examined.

RESULTS

Polybutadiene

The in-phase Young's modulus and loss factor for polybutadiene are given in *Figures 3* and *4*. These results were obtained from longitudinal vibration tests and forced non-resonance tests on compression buttons. For the latter, results are reported up to 600 Hz at which frequency the error in the force signal due to machine vibration was of the order of 0.5%. The effect of the shape factor was taken into account when calculating the modulus of the rubber. The in-phase Young's modulus and loss factor deduced from the longitudinal resonance tests show a rapid change at frequencies above 1800 Hz. In this region, the wavelength of the propagating wave is becoming comparable to the lateral dimensions of the sample and therefore the plane wave analysis used is no longer appropriate.

Natural Rubber

The dynamic shear modulus and loss factor for a natural rubber vulcanisate (B) at 22°C are shown as functions of frequency in *Figures 5* and *6*. For the longitudinal resonance tests, the shear modulus ($G = E/3$) and loss factor are reported up to 1500 Hz at which frequency the ratio of the wavelength to the cross-sectional dimension (~ 5 mm) was $\sim 6:1$. These results appear to be reasonably reproducible and independent of the length of the sample over the range 176 mm to 67 mm.

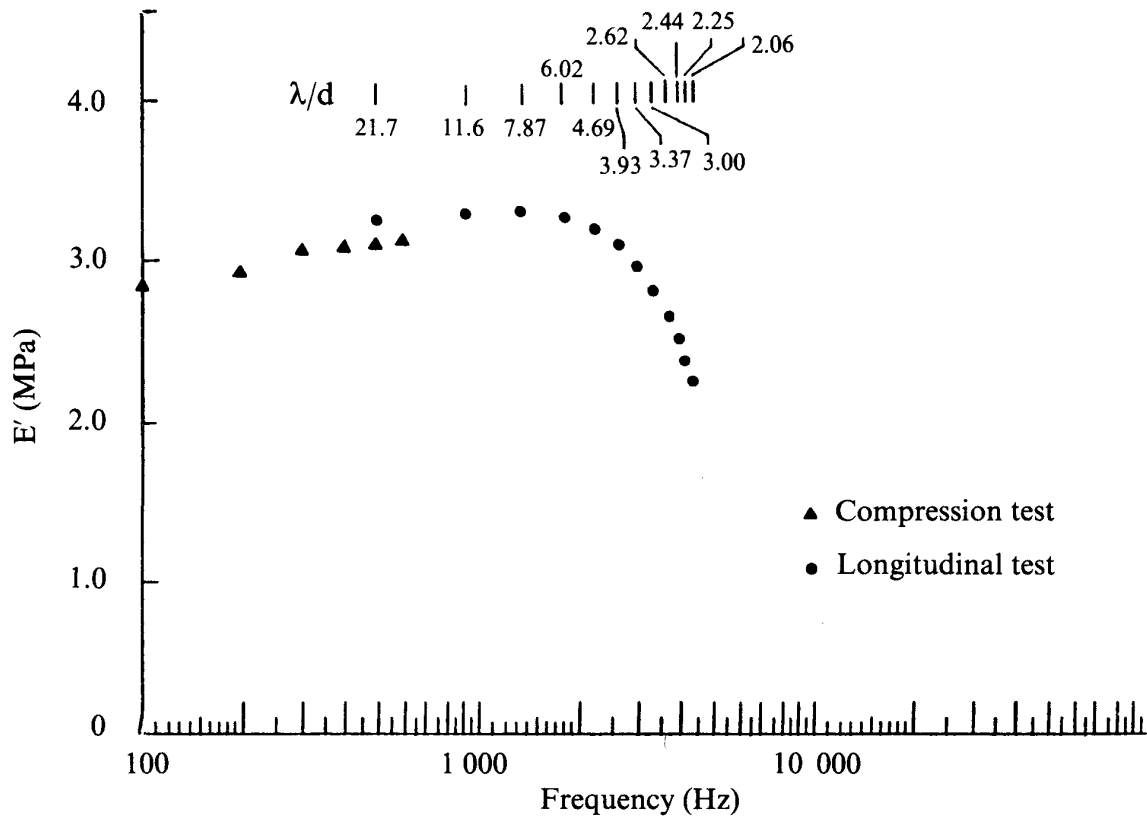


Figure 3. Variation of in-phase Young's modulus with frequency at ambient temperature (22°C) for Vulcanisate A. The ratio of the wavelength λ to lateral dimension d ($= 5$ mm) is also shown. Sample length for the longitudinal test was 64 mm.

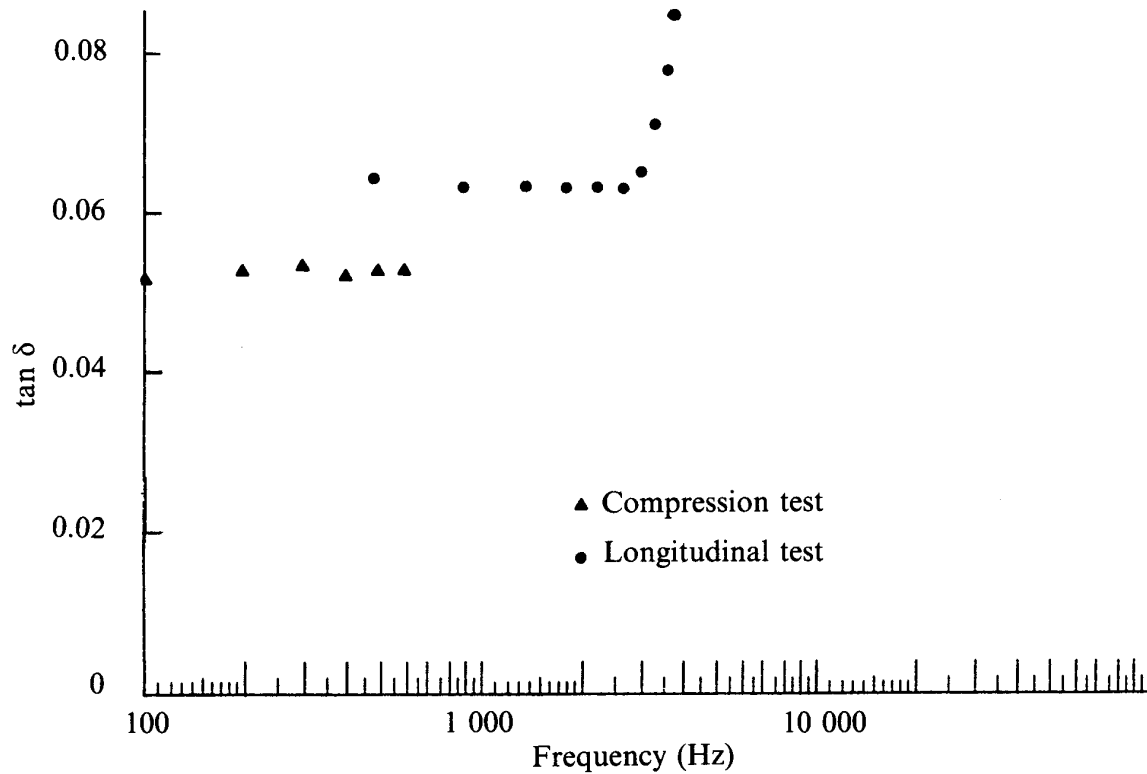


Figure 4. Variation of loss factor with frequency for Vulcanisate A.

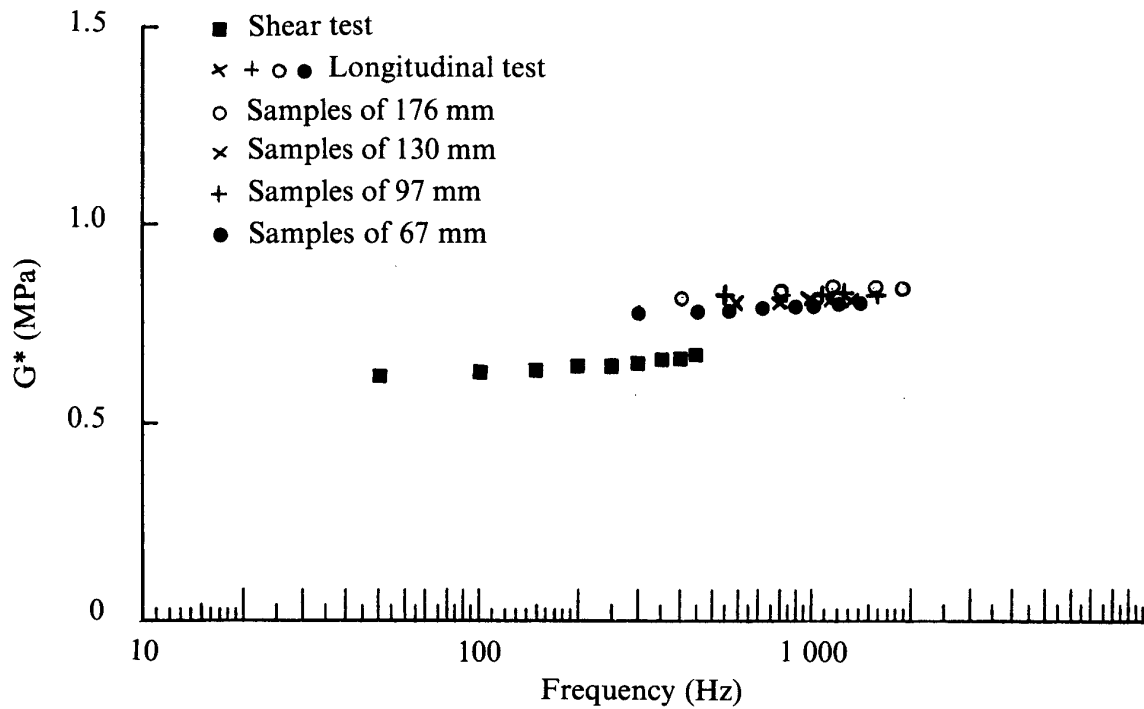


Figure 5. Dependence of G^* on frequency for Vulcanisate B at 22°C . Samples of 176 mm, 130 mm, 97 mm and 67 mm length were used for the longitudinal vibration test.

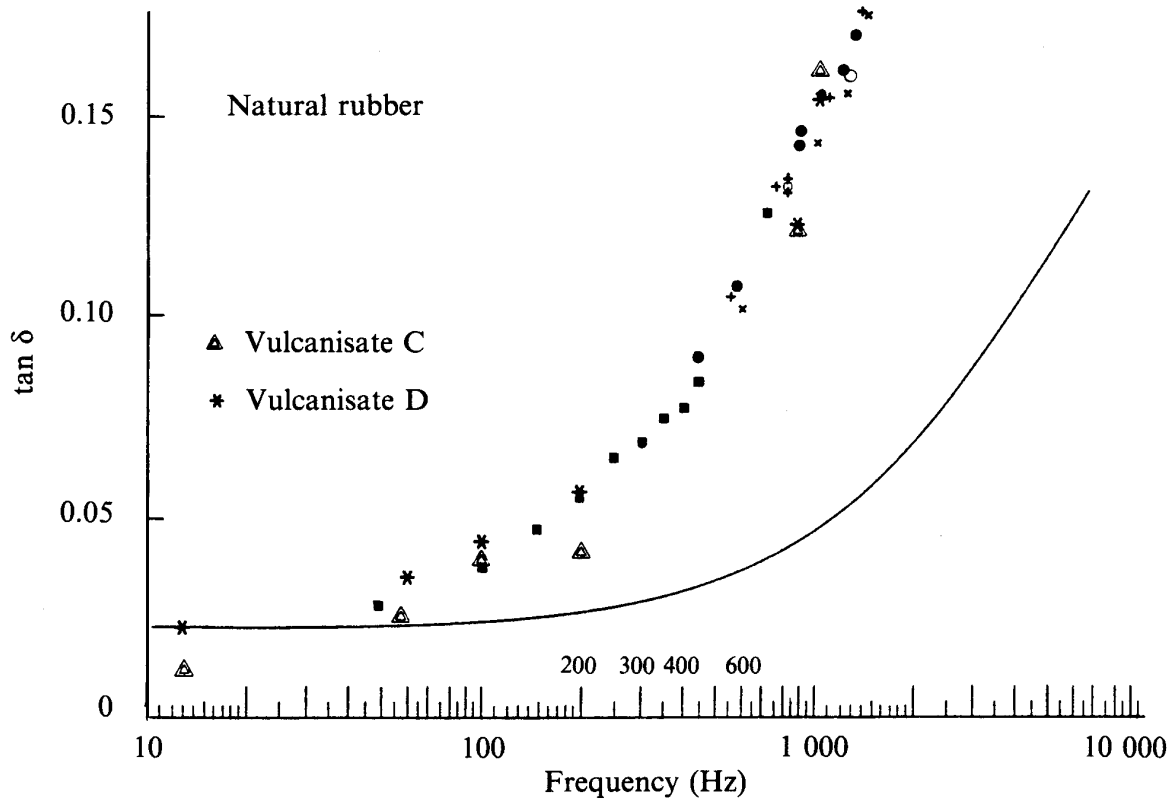


Figure 6. Dependence of $\tan \delta$ on frequency for Vulcanisate B at 22°C . The solid curve is the Fletcher and Gent data transformed to 22°C . $T_S = -21^\circ\text{C}$. Also shown is the data for Vulcanisates C and D from EDS series transformed to this temperature using the same reference temperature, T_S .

Time-temperature Equivalence Principle

The effects of temperature and frequency on the response of polymers to mechanical oscillations can be inter-related at temperatures above the glass transition. Temperature affects all relaxation times similarly and therefore an equivalence exists between a change in the frequency of oscillations and a change in temperature. If the relaxation times are increased by a factor a_T when the temperature is changed from T_S to T , the in-phase shear modulus at a frequency f and temperature T is given by:

$$G'(f, T) = \frac{T\rho}{T_S \rho_S} G'(fa_T, T_S)$$

where ρ and ρ_S are the density at temperatures T and T_S respectively. The loss factor $\tan \delta$ is given by

$$\tan [\delta(f, T)] = \tan [\delta(fa_T, T_S)]$$

The factor a_T gives a measure of the temperature dependence of the relaxation times. The following expression for a_T has been found to apply reasonably accurately to many polymers provided a value for the reference temperature, T_S , appropriate to each polymer is chosen².

$$\log_{10} a_T = -8.86 (T - T_S) / [101.6 + (T - T_S)] \quad \dots 6$$

This relationship has been found to work in the range of $T_S \pm 50^\circ\text{C}$. A reasonable estimate for T_S is given by $T_S \approx T_g + 50^\circ\text{C}$ where T_g is the glass transition temperature.

Figure 6 also shows the trend of previously reported values of $\tan \delta$ for a vulcanisate of the same formulation as *Vulcanisate B*. The original measured values have been transformed to this frequency range by using the time-temperature equivalence principle. The data had been obtained from double shear test-pieces (25 mm diameter and 6.4 mm in height) deformed sinusoidally with a shear amplitude of $\sim 2\%$ strain. The tests were carried out at frequencies from 1.6×10^{-3} Hz to 4.8 Hz for temperatures in

the range of -62°C to 81.5°C . The reference temperature¹ for this vulcanisate was reported to be $T_S = -21^\circ\text{C}$. The data were reduced to 22°C in Figure 6 using the same value.

The dynamic shear modulus and $\tan \delta$ for *Vulcanisates C* and *D* are shown as a function of frequency in Figure 7. These are unfilled natural rubber vulcanisates each with a similar curing system to *Vulcanisate B*. The original data were obtained in simple shear⁴ at three frequencies (0.1, 1 and 15 Hz) at a strain of 2% and for temperatures between -40°C and 150°C . Data in Figure 7 has been transformed to 22°C using Equation 6. The reference temperature used was -21°C ; the values of shear modulus have not been adjusted to take account of the dependence on temperature predicted by the kinetic theory of rubber elasticity.

DISCUSSION

Below 1800 Hz, the dynamic properties of polybutadiene appear, as expected, insensitive to the frequency of deformation (*Figures 3 and 4*). The apparent strong frequency sensitivity of the dynamic properties of the polybutadiene at frequencies above 1800 Hz is inconsistent with the expected behaviour. The reason for this is thought to be that the analysis is only applicable at frequencies where the wavelength of the propagating wave is large compared with the lateral dimensions of the sample. The results indicate that the longitudinal vibration method may be reliable provided this condition is satisfied.

Figures 5 and 7 indicate that the dynamic modulus of unfilled NR is fairly constant at room temperature up to 1500 Hz. The longitudinal vibration method, however, gave a higher level of modulus for both polybutadiene and natural rubber than that obtained by the forced non-resonance method in simple shear or compression. The reason for the discrepancy is not clear. The quasi-static shear modulus of the natural rubber rod used in the longitudinal

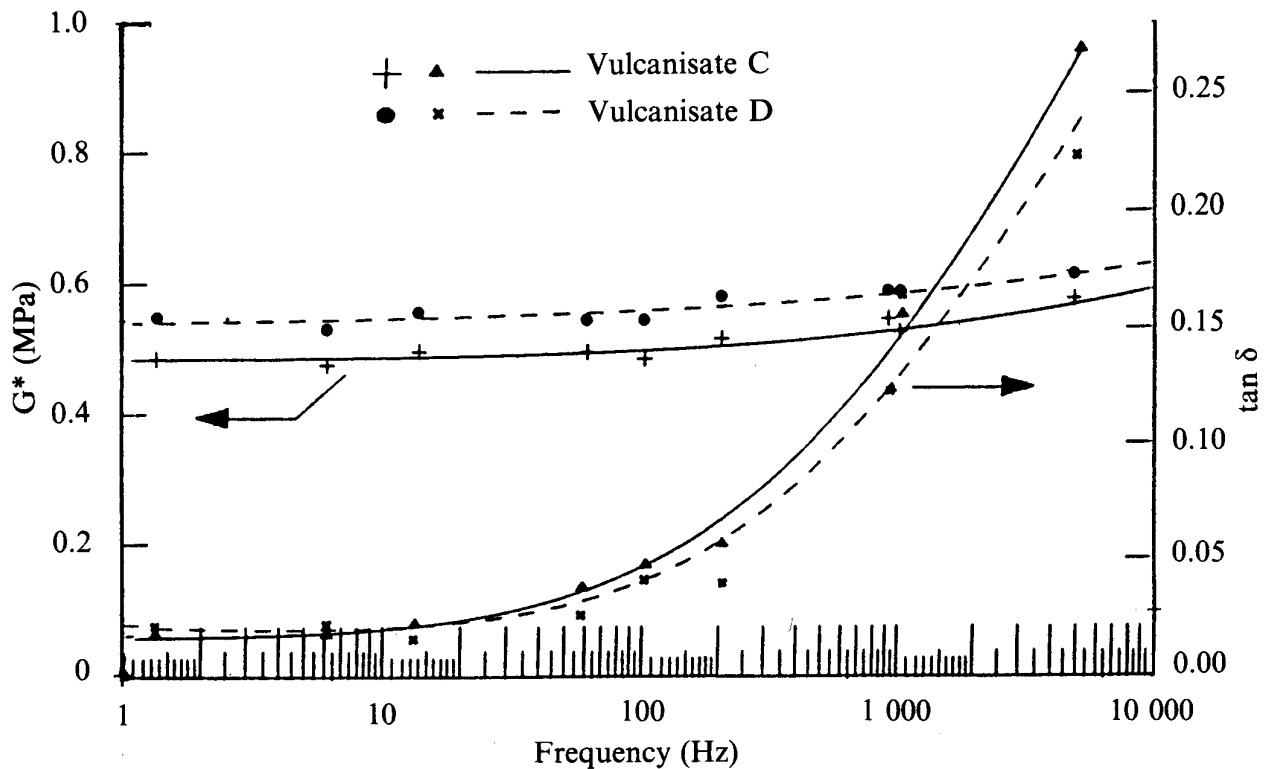


Figure 7. Variation of G^* and $\tan \delta$ with frequency for Vulcanisates C and D using EDS data transformed to 22°C with $T_s = -21^\circ\text{C}$.

vibration tests agreed closely with the value obtained in simple shear by the non-resonance method.

The directly measured properties of a natural rubber vulcanisate at high frequencies show a greater dependence of the loss factor on frequency at ambient temperature than indicated, for a nominally similar compound, by the data of Fletcher and Gent¹, as transformed by the time-temperature equivalence principle. It is believed that the dependence of loss factor of natural rubber on frequency, evident in Figure 6, cannot simply be an artefact of the techniques, since no such dependence was observed for polybutadiene (Figure 4). Moreover, the data given in Engineering Data Sheet⁴ for two vulcanisates having similar cure systems to Vulcanisate B show, when transformed, the same frequency dependence for loss factor as the present directly measured data (Figure 7). For

comparison, this data is also plotted in Figure 6. It is possible that given the type of curing system used, the level of $\tan \delta$ for Vulcanisates C and D could have been raised due to their longer curing times compared with that for Vulcanisate B. However, it appears unlikely that this effect could account for the differences observed between the loss factors from the EDS data and those from Fletcher and Gent. Furthermore, the fact that both the EDS data and Fletcher and Gent's data have been shifted to about the same extent along the frequency axis, rules out the large magnitude of the shift as a possible explanation for the discrepancy between the directly measured data and those based on Fletcher and Gent's results.

CONCLUSIONS

The longitudinal vibration method can be used to measure the dynamic properties of

elastomers with low loss factor, such as natural rubber. An upper limit on the frequency is set by the sample dimension and the speed of propagating waves in the material.

The dynamic modulus for the unfilled natural rubber vulcanisate tested is relatively unchanged up to 2 kHz whereas its loss factor rises considerably in this region. Given the agreement between the direct measurements and the transformed EDS data, it seems more likely that the original Fletcher and Gent results were inaccurate, and that data transformed according to the time-temperature equivalence principle give as accurate an indication of high frequency behaviour as directly measured data.

Date of receipt: April 1992

Date of acceptance: July 1992

REFERENCES

1. FLETCHER, W.P. AND GENT, A.N. (1957) Dynamic Shear Properties of Some Rubber-like Materials. *Br. J. appl. Phys.*, **8**, 194.
2. WILLIAMS, M.L., LANDEL, R.F. AND FERRY, J.D. (1955) The Temperature Dependence of Relaxation Mechanisms in Amorphous Polymers and Other Glass-forming Liquids. *J. Am. chem. Soc.*, **77**, 3701.
3. AHMADI, H.R. AND MUHR, A.H. (1992) Vibration Control using Rubber Components. *Int. J. Mater. Prod. Technol.*, **7**(1).
4. MALAYSIAN RUBBER PRODUCERS' RESEARCH ASSOCIATION (1979) *Natural Rubber Engineering Data Sheet*.
5. LEE, T.M. (1963) Method of Determining Dynamic Properties of Viscoelastic Solids Employing Forced Vibration. *J. appl. Phys.*, **20**, 481.
6. NORRIS, JR., D.M. AND YOUNG, W.C. (1970) Complex Modulus Measurement by Longitudinal Vibration Testing. *Expl Mech.*, **10**, 93.
7. LOVE, A.E.H. (1927) *The Mathematical Theory of Elasticity* (4th edition), p.287. Cambridge: University Press.
8. BRADFIELD, G. (1964) Use in Industry of Elasticity Measurements in Metals with the Help of Mechanical Vibrations. National Physical Laboratory, HMSO, London.
9. GENT, A.N. AND LINDLEY, P.B. (1959) The Compression of Bonded Rubber Blocks. *Proc. Instn mech. Engrs*, **173**, 111.
10. READ, B.E. AND DEAN, G.D. (1978) *The Determination of Dynamic Properties of Polymers and Composites*. Bristol: Adam Hilger Ltd.
11. BRITISH STANDARDS INSTITUTION (1976) Measurement of Dynamic Moduli. BS903: Part A24.

APPENDIX 1

Compound	A	B	C	D
<i>Cis</i> BR (Europrene <i>cis</i>)	100			
Natural rubber (smoked sheet)		100		
Natural rubber (SMR CV60)			100	100
Dicumyl peroxide	0.5			
CBS		0.8	0.6	0.8
Sulphur		2.5	2.5	3.25
Zinc oxide		5	5	5
Stearic acid		2	2	2
HPPD				3
Antioxidant, TMQ			2	
Antiozonant, DOPD			4	
Wax				2
Vulcanisation temperature (°C)	150	140	140	140
Vulcanisation time (min)	70	30	45	45

The amount of each ingredient is given in parts by weight.

- CBS N-cyclohexyl benzothiazole-2-sulphenamide
- HPPD N-(1,3-dimethylbutyl)-N'-phenyl-p-phenylenediamine
- TMQ Polymerised 2,2,4-trimethyl-1,2-dihydroquinoline
- DOPD N, N'-di-(1-ethyl-3-methylpentyl)-p-phenylenediamine

APPENDIX 2

Testing in shear could be represented as shown in *Figure A1*.

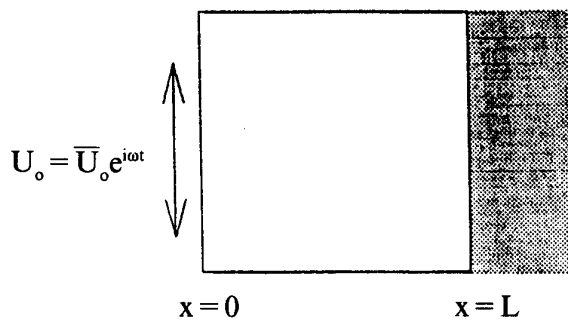


Figure A1.

The displacement $U_o = \bar{U}_o e^{i\omega t}$ is applied at the face $x=0$ and the force is measured at $x=L$. At frequencies well below the

resonance of the sample, the displacement at any point along the sample is given by:

$$U_o(x, t) = \bar{U}_o \left(1 - \frac{x}{L}\right) e^{i\omega t} \quad \dots A1$$

the measured force at $x=L$ is

$$F^* = \frac{AG^*}{L} \bar{U}_o e^{i\omega t} = \bar{F}_o e^{i(\omega t + \delta)} \quad \dots A2$$

where A is the cross-sectional area, G^* is the complex shear modulus, and δ the loss angle.

The dynamic modulus G is given by:

$$G = \frac{\bar{F}_o}{\bar{U}_o} \frac{L}{A} \quad \dots A3$$

When the driving frequency approaches the sample's resonant frequency, the displace-

ment distribution is no longer represented by Equation A1, and a propagating wave solution is required. The theory for the propagation of plane waves along the x-axis is used with boundary conditions of:

$$U^*(x) = \bar{U}_o \quad \text{at } x = 0$$

$$= 0 \quad \text{at } x = L$$

The measured force at $x=L$ is related to the applied displacement U_o as follows:

$$F^* = GA \left. \frac{\partial U}{\partial x} \right|_{x=L} = \bar{F}_o e^{i(\omega t + \theta)}$$

$$= \frac{AG^* c^* L}{L \sin c^* L} \bar{U}_o e^{i\omega t} \quad \dots A 4$$

where $c^* = (\omega^2 \rho / G^*)^{1/2}$, and θ is the phase difference between the force and displacement signal.

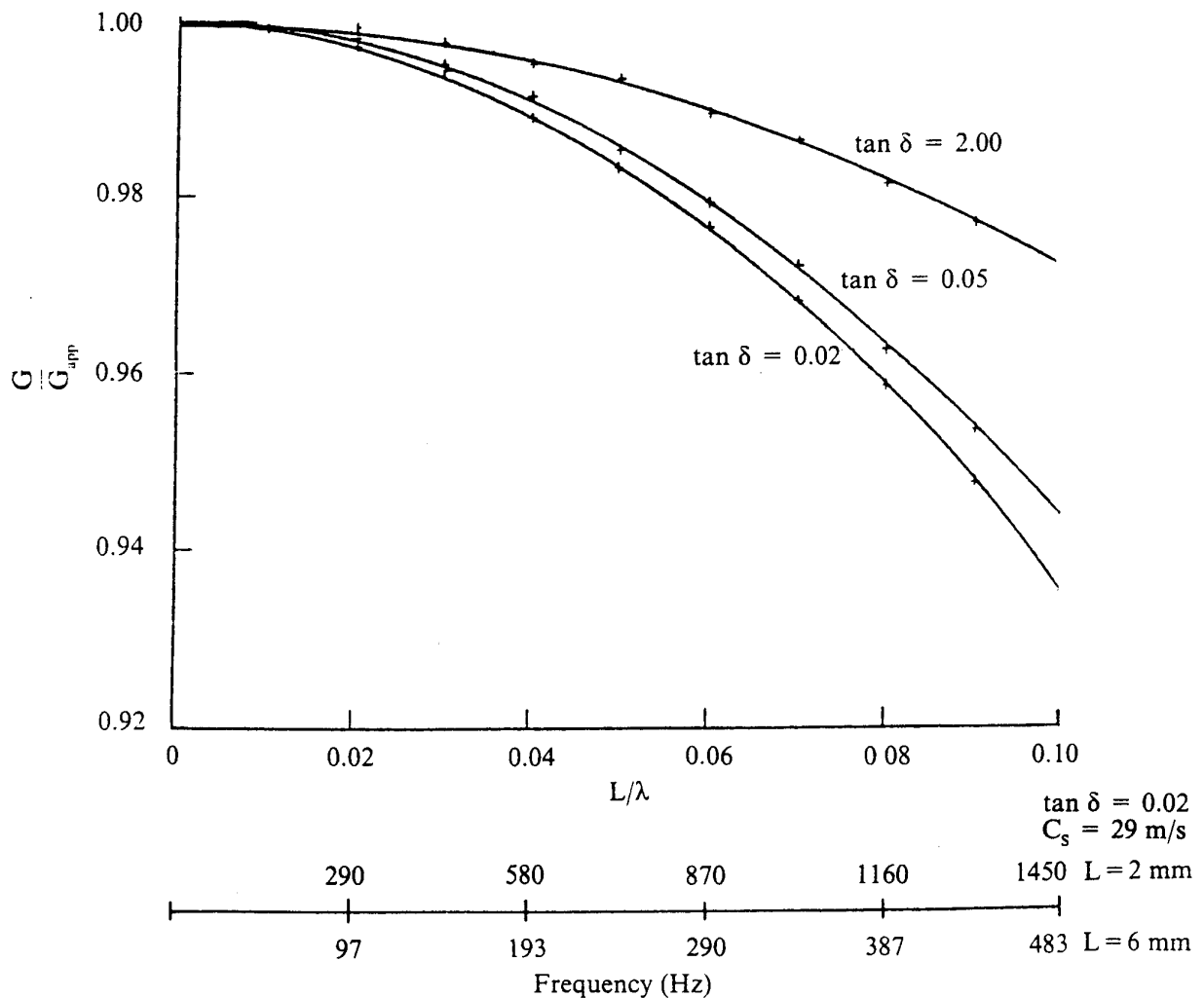


Figure A2. Dependence of the ratio of the dynamic shear modulus to the apparent dynamic modulus ($G/G_{apparent}$) on the ratio of the length of the sample to the wavelength of the propagating wave (L/λ). The loss factor of the material is the parameter. First resonance occurs at $L/\lambda = 0.5$. Also shown are corresponding frequency scales for two natural rubber samples of 2 mm and 6 mm length. Temperature = 22°C and constant $\tan \delta = 0.02$.

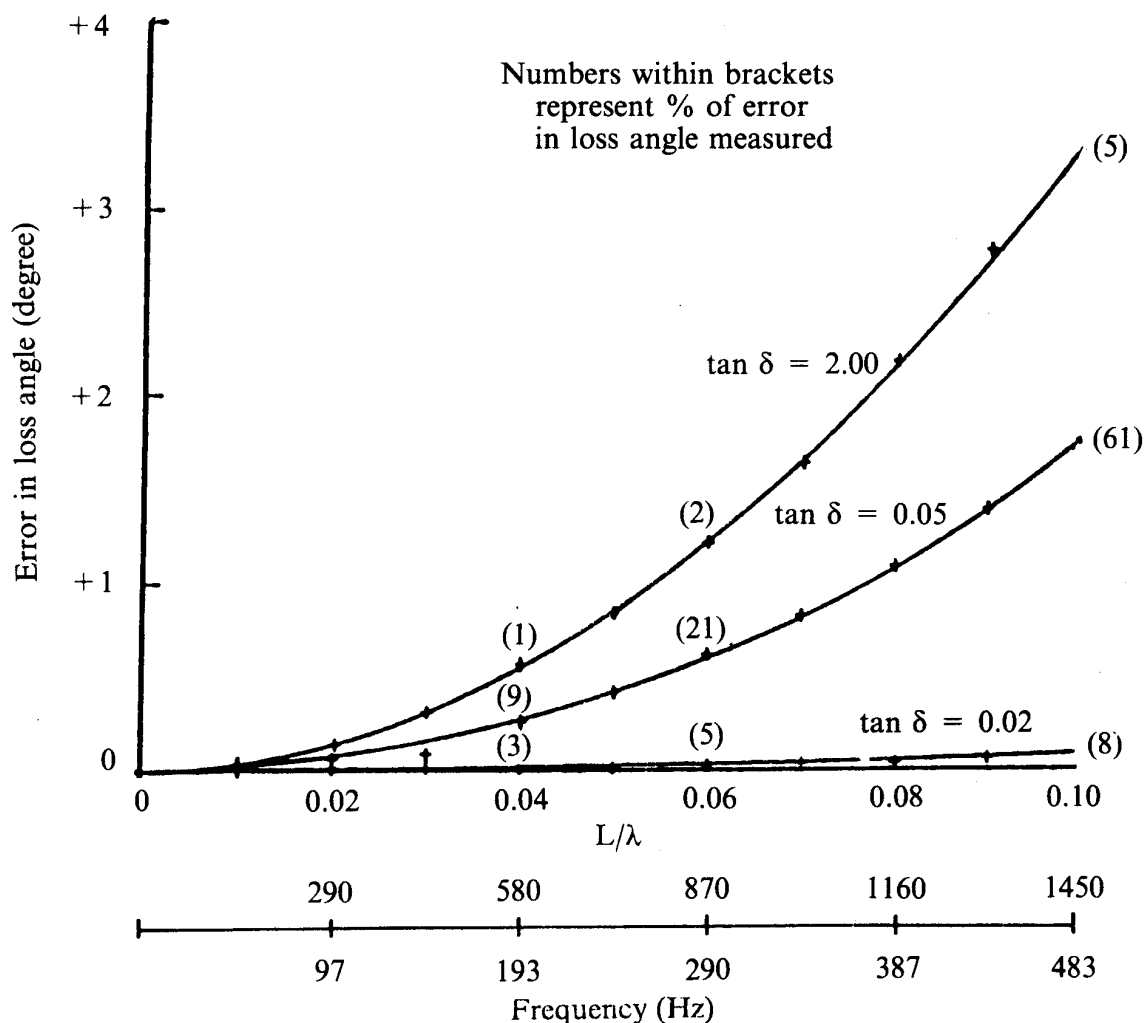


Figure A3. Variation of the error in the measured loss angle with L/λ .

Therefore the material's dynamic modulus and loss angle are given by:

$$G = G_{\text{apparent}} \left| \frac{\sin c^*L}{c^*L} \right| \quad \dots A5$$

$$\delta = \delta_{\text{apparent}} + \arg \left(\frac{\sin c^*L}{c^*L} \right) \quad \dots A6$$

where G_{apparent} is the modulus as given by Equation A3 and δ_{apparent} is θ .

Figures A2 and A3 show plots of $|\sin c^*L/c^*L|$ and $\arg(\sin c^*L/c^*L)$ against the ratio of the sample length L to the wavelength of the propagating wave λ , with $\tan \delta$ as a parameter.